arXiv:2402.17829v1

The evolution of the SFR and Σ_{SFR} of galaxies in cosmic morning ($4 < z < 10$)

ABSTRACT

The galaxy integrated star-formation rate (SFR) surface density (Σ_{SFR}) has been proposed as a valuable diagnostic of the mass accumulation in galaxies as being more tightly related to the physics of star-formation and stellar feedback than other star-formation indicators. In this paper, we assemble a statistical sample of 230 galaxies observed with JWST in the GLASS and CEERS spectroscopic surveys to estimate Balmer line based dust attenuations and SFRs (i.e., from Hα, Hβ, and Hγ), and UV rest-frame effective radii. We study the evolution of galaxy SFR and Σ_{SFR} in the first 1.5 Billion years of our Universe, from redshift $z \sim 4$ to $z \sim 10$. We find that Σ_{SFR} is mildly increasing with redshift with a linear slope of 0.16 ± 0.06. We explore the dependence of SFR and Σ_{SFR} on stellar mass, showing that a star-forming 'Main-Sequence' and a Σ_{SFR} 'Main-Sequence' are in place out to $z = 10$, with a similar slope compared to the same relations at lower redshifts, but with a higher normalization. We find that the specific SFR (sSFR) and Σ_{SFR} are correlated with the [O III] λ5007Å/[O II] λ3727Å ratio and with indirect estimates of the escape fraction of Lyman continuum photons, hence they likely play an important role in the evolution of ionization conditions at higher redshifts and in the escape of ionizing radiation. We also search for spectral outflow signatures in the Hα and [O III] emission lines in a subset of galaxies observed at high resolution (R= 2700) by the GLASS survey, finding an outflow incidence of 2/11 (= $20\%^{32\%}_{9\%}$) at $z < 6$, but no evidence at $z > 6$ (0/6, < 26%). Finally, we find a positive correlation between A_V and Σ_{SFR}, and a flat trend as a function of sSFR, indicating that there is no evidence of a drop of A_V in extremely star-forming galaxies between $z \sim 4$ and ~ 10. This might be at odds with a dust-clearing outflow scenario, which might instead take place at redshifts $z \geq 10$, as suggested by some theoretical models.

- Estimate Balmer line based dust attenuations and SFRs (i.e., from Hα, Hβ, and Hγ), and UV rest-frame effective radii.
- ΣSFR is mildly increasing with redshift with a linear slope of 0.16 ± 0.06.
- Star-forming main sequence and a ΣSFR main sequence are in place out to z = 10.
- Specific SFR (sSFR) and ΣSFR are correlated with the [O iii] λ5007Å/[O ii] λ3727Å ratio and with indirect estimates of the escape fraction of Lyman continuum photons.
- There is no evidence of a drop of A_V in extremely star-forming galaxies between z ~ 4 and ~ 10.

1. Introduction

- Star formation rate (SFR): link to galaxy properties such as stellar mass from main sequence.
- ΣSFR : surface density of star-formation.

Definition) This quantity represents the SFR normalized by the surface area where it occurs, and encapsulates information about the spatial distribution of star formation.

- Why ΣSFR is important ?
  -> As galaxies become increasingly more compact at higher redshifts, since the dependence on the size is quadratic, ΣSFR increases more rapidly with redshift compared to the sSFR.
- ΣSFR = SFR / ($2\pi \times r^2_e$) , where r_e is the half-light radius.

JWST can resolve galaxy sizes out to the epoch of reionization.
  -> We can derive r_e (half-light radius)

- Goal: to investigate how the SFR and the SFR surface density (ΣSFR) evolve in the first 1.5 Billion years of our Universe.

2. Data and method

- Data: JWST-GLASS and JWST-CEERS

2.1. Spectroscopic observations and sample selection

- Targeted galaxies: residing over the central regions of the Abell 2744
  - Since GLASS-JWST observations target sources behind a lensing cluster, they adopt the global properties such as stellar masses, line fluxes, SFRs, and galaxy sizes for magnification effects.
- Select data: spectroscopic redshift z > 4 from NIRSpec data

2.2. Line measurements and derivation of star-formation rates

- To fit rest-frame optical emission lines by using χ2 minimization: [O ii] λ3727Å, Hγ, [O iii] λ5007Å, Hβ, and Hα.
  -> The fit of the emission lines yields the redshift of the sources, the line widths, the line fluxes, and their corresponding uncertainties.

2.3. Derive SFR and SFR surface density

- 1) Compute the gas-phase attenuation A_V from the available Balmer lines (among Hγ , Hβ, and Hα)
  - If only one Balmer line is detected, they adopt an A_V as inferred from the SED fitting procedure.
- 2) Derive the star formation rates
  - Compute the observed, dust-corrected Hα luminosity ($L_{H\alpha}$).
  - If Hα is not detected, consider the fluxes of Hβ (or Hγ as last possibility)
  - Intrinsic ratios of 2.86 and 6.10 respectively for Hβ and Hγ
  - Sample data to derive SFR: from Hα in 153 galaxies, from Hβ in 67 systems, while for 10 galaxies it is inferred from Hγ
- 3) Convert $L_{H\alpha}$ to SFR assuming the calibration of Reddy et al.
  - SFR = $L_{H\alpha} \times 10^{-41.67}$.
- 4) Derive stellar masses of galaxies: through an SED fitting procedure using the code cigale (Boquien et al. 2019)
- 5) Galaxy sizes and SFR surface density estimation
  - Measure the major-axis half-light radius r_e of our galaxies by fitting with the python software galight (Ding et al. 2021)
  - Their rest-frame UV images because of tracing star formation from the emission of young massive stars.

3. Result

3.1 Fitting methods

black empty diamonds: median redshift and the median ΣSFR of galaxies

3.2. The redshift evolution of the SFR surface density

- Mild evolution of ΣSFR from z ≃ 4 to z ~ 8,
- Best-fit slopes: 0.16 ± 0.06

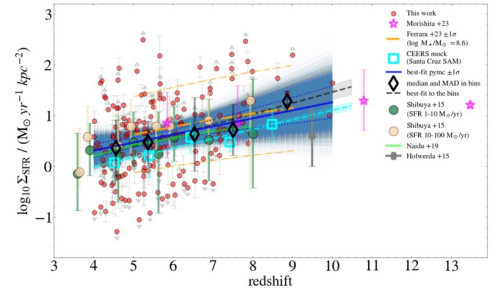

[Figure 1]. Redshift evolution of ΣSFR from z = 4 to 10

3.3. The main sequence of star-formation at z > 4

- SFMS in the two redshift bins have similar slopes
  - SFMS slope at 4 < z < 6: 0.7 ± 0.06
  - SFMS slope at 6 < z < 10: 0.76 ± 0.08

3.4. The main sequence of SFR surface density

- ΣSFR is approximately constant across the Main Sequence.
- ΣSFR slightly increasing in more massive galaxies.
  - slope at 4 < z < 6: 0.19 ± 0.09
  - slope at 6 < z < 10: 0.30 ± 0.15

4. Discussion

4.1. SFR surface density and ionization properties

- Reddy et al. (2022): SFR surface densities of galaxies have been shown to be tightly related and to have a key influence on their ionizing properties

$$O32 = (0.415 \pm 0.064)\log[\Sigma_{SFR}/M_\odot\ \mathrm{yr}^{-1}\,\mathrm{kpc}^{-2}] + 0.307 \pm 0.030$$

  -> See how this relationship changes in high redshift galaxies
- Slope of 1.5 ± 0.2
- Galaxies in the top right part of the diagram, with ΣSFR ≥ 1 and O32 ≥ 0.7, have similar properties to photometrically selected extreme emission line galaxies (EELGs) in the CEERS field at z = 4-9
- Lyman continuum leaking sources (LyC): to have higher ΣSFR than the average value of the star-forming population

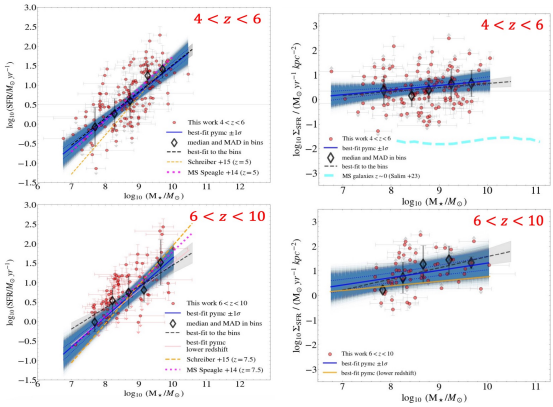

[Figure 2]. Star-forming main sequence plot, comparison at 4<z<6 and 6<z<10 epoch between star formation rate and stellar mass of galaxy (left), ΣSFR and stellar mass of galaxy (right).

4.2. Investigating attenuation A_V

- How the galaxy attenuation A_V is related to the star-forming properties?
  - Galaxies at z > 7 have a large variety of A_V (Figure 4).
- A_V vs sSFR (Figure 5)
  - higher sSFR show a large variety of A_V.
  - median A_V slightly increases with sSFR, but almost flat relation (slope: 0.07 ± 0.09).
- A_V vs Σ SFR (Figure 6)
  - best-fit slope: 0.28 ± 0.07
  - indicate that galaxies with more concentrated star-formation (i.e., higher ΣSFR) have higher dust attenuation.
  - This correlation is similar to in lower redshift studies

5. Summary

- Spectroscopic sample of galaxies in the redshift range from 4 to 10 observed with JWST-NIRSpec by the CEERS and GLASS surveys
- Using the Balmer lines and UV-based effective radii, they derive the SFR and ΣSFR
- ΣSFR increases mildly in this redshift range (best-fit slope = 0.16 ± 0.06), rising by a factor of 2 from z = 4 to 10.
- A star-forming main sequence relation holds out to redshift ~ 10, with a best-fit slope of ~ 0.7
- Derive for the first time at z > 4 the ΣSFR 'Main Sequence', finding a very mild increase (consistent with a flat relation) of ΣSFR with stellar mass.
- Find a positive correlation between A_V and ΣSFR , and a flat trend as a function of sSFR, indicating that there is no evidence of a drop of AV in extremely star-forming galaxies between z = 4 and 10.

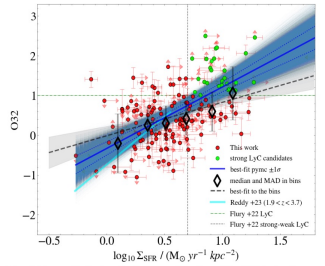

[Figure 3]. The ΣSFR as a function of the O32 index for selected sample in the entire range 4 < z < 10.

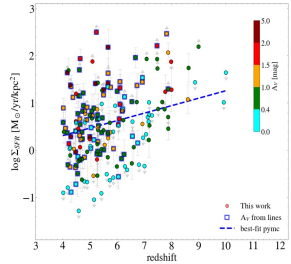

[Figure 4]. Redshift and ΣSFR diagram as a function of attenuation A_V.

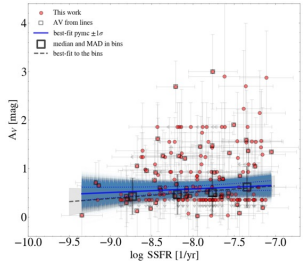

[Figure 5]. A_V as a function of sSFR for the entire redshift range

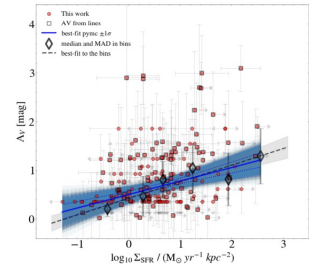

[Figure 6]. A_V as a function of ΣSFR for the entire redshift range